Research Square

Preprints are preliminary reports that have not undergone peer review.
They should not be considered conclusive, used to inform clinical practice,
or referenced by the media as validated information.

Sample-to-answer automated centrifugal microfluidics with computer-vision readout for point-of-care molecular diagnostics

Ahmad S. Akhtar

asakhtar@kth.se

KTH Royal Institute of Technology

Noa Lapins

KTH Royal Institute of Technology

João M. Moura

INL – International Iberian Nanotechnology Laboratory

Luis Paula

INL – International Iberian Nanotechnology Laboratory

Adriano Pedro

INL – International Iberian Nanotechnology Laboratory

Fabio Martins

INL – International Iberian Nanotechnology Laboratory

Duarte Mota

INL – International Iberian Nanotechnology Laboratory

Inês F. Pinto

KTH Royal Institute of Technology

Marco Martins

INL – International Iberian Nanotechnology Laboratory

Aman Russom

KTH Royal Institute of Technology

Research Article

Keywords: Centrifugal microfluidics, Point-of-care diagnostics, Loop-mediated isothermal amplification (LAMP), Computer vision, Automation

Posted Date: November 2nd, 2026

DOI: https://doi.org/10.21203/rs.3.rs-11174292/v1

License: This work is licensed under a Creative Commons Attribution 4.0 International License.
Read Full License

Additional Declarations: No competing interests reported.

Abstract

The COVID-19 pandemic exposed how unprepared the world is to respond to an infectious disease outbreak at scale. Conventional diagnostic testing relies on centralized laboratories, and when testing demand surges during an outbreak, these facilities become strained for resources and personnel, a problem compounded in low- and middle-income countries with less developed health and transport infrastructure. Decentralized, point-of-care diagnostics offer a path around this bottleneck, but automated platforms capable of true sample-to-answer operation remain limited. Here we report a fully automated centrifugal microfluidic platform that combines loop-mediated isothermal amplification (LAMP) with computer-vision-based readout, demonstrated using SARS-CoV-2 detection as a model application. The integrated platform performs the complete assay protocol, including heating, rotation, and optical detection, at the push of a single button, without user intervention, processing 26 samples in 40 minutes. Using RNA fragments spiked into water and artificial saliva, the platform consistently detected amplification down to approximately 1000 copies per 10 µL reaction. This platform architecture is broadly applicable beyond SARS-CoV-2 and offers a template for rapid, decentralized molecular diagnostics for future infectious disease outbreaks.

1. Introduction

The COVID-19 pandemic exposed a persistent gap in global capacity for infectious disease diagnostics: testing infrastructure that had historically been limited to central laboratories and hospitals proved unable to scale to the demands of population-level screening (Peeling and Sia, 2023, Wong et al., 2025, Tupps et al., 2025, Lu et al., 2025, Rakeman-Cagno et al., 2024). As countries relied on mass testing to keep schools, workplaces, and other public spaces operating safely, diagnostics took on a role well beyond its traditional use in managing individual illness (Peeling and Sia, 2023, Rakeman-Cagno et al., 2024). This exposed the need for testing methods that do not depend on specialized equipment or trained personnel, a need that remains relevant beyond COVID-19 for any future outbreak of an emerging pathogen (Wong et al., 2025, Rutter et al., 2026, Lu et al., 2025, Rakeman-Cagno et al., 2024, Yimer et al., 2024).

In the initial stages of COVID-19, nucleic acid tests were used for mass screening, but as the burden on healthcare systems grew and reagent and supply shortages worsened, antigen tests were approved for home use, allowing people to self-isolate based on a positive result (Peeling and Sia, 2023, Lu et al., 2025). Rapid antigen tests are easy to use, requiring no prior technical expertise and giving rapid results, but their lower sensitivity and specificity make them unsuitable as a frontline diagnostic method (Lu et al., 2025). Among nucleic acid testing methods, polymerase chain reaction (PCR) has been the gold standard since its inception and was the method of choice for clinical diagnosis of COVID-19, followed by isolation or quarantine to limit transmission. PCR requires precise temperature cycling, which typically demands expensive equipment and limits its use to centralized laboratories (Lu et al., 2025, Yimer et al., 2024). Isothermal amplification methods circumvent this limitation by amplifying nucleic acids at a

constant temperature, making them easier to integrate into point-of-care devices (Novi et al., 2025, Bi et al., 2025, Jirakittiwut and Ratthawongjirakul, 2025).

For nucleic acid amplification, sample collection is followed by pre-treatment to purify the sample and remove any inhibitors that might interfere with amplification (Wang et al., 2023, Narasimhan et al., 2023, Justo et al., 2025, Cunha et al., 2021). This pre-treatment step varies with sample type and amplification method, and adds complexity in terms of equipment, time, and technical expertise (Cunha et al., 2021, Chakraborty, 2024, AbdElFatah et al., 2023). One approach to this problem is to simplify and/or integrate the sample preparation step directly into the diagnostic device, focusing on pathogens or biomarkers detectable from samples that are easy to collect and require minimal processing. In this context, saliva was explored as an alternative to nasopharyngeal swabs, since swab collection is invasive and requires a trained healthcare worker whereas saliva sample can be collected even at home or workplace making it suitable for mass screening and/or point-of-care testing (Kumari et al., 2023). Several studies showed that saliva samples can be used for nucleic acid amplification following a simple heat-inactivation step, eliminating the need for a lengthy extraction step (Sritong et al., 2024, Varughese et al., 2025, Peno et al., 2024, Margulis et al., 2024, Jenkins et al., 2022, Vogels et al., 2021, Zhang et al., 2021). Furthermore, saliva has also been reported as a feasible diagnostic sample for tuberculosis (Tang et al., 2023, Byanyima et al., 2022) and other respiratory pathogens (Lee et al., 2022, Kshirsagar et al., 2025, Hernaez et al., 2023).

Here, we present a fully automated centrifugal microfluidic platform for sample-to-answer molecular diagnostics, demonstrated using artificial saliva samples for SARS-CoV-2 detection. The platform automates and performs all steps from sample loading to detection at the push of a button, without requiring user intervention. We previously reported a low-cost integrated centrifugal microfluidic platform for COVID-19 diagnosis that combined RT-LAMP with a novel bead-based strategy for fluorescence signal enhancement and a simple smartphone-based readout (Soares et al., 2021). It still required the user to manually move the centrifugal disc between the heating system and the rotor to complete the reaction, and to individually image each channel with a smartphone. The platform reported here carries out heating, rotation, and detection at a single position in a fully automated manner, using a lifting mechanism that brings the disc into contact with the heater for amplification and then lifts it for rotation and detection. Detection is performed automatically using computer vision, which identifies each channel and measures fluorescence in the corresponding detection chamber. The heating module has also been redesigned, reducing power consumption enough to make the system fully battery operable. Although demonstrated here for SARS-CoV-2, this platform architecture is directly transferable to other LAMP-compatible targets, making it a general tool for decentralized outbreak response.

2. Methods

2.1. Fabrication and assembly of centrifugal microfluidic discs

The centrifugal disc was designed using Autodesk® Fusion 360 software (Education License). Each disc is made up of three layers: (i) top disc which is cut from a 2 mm thick clear PMMA sheet; (ii) middle layer of 50 μm thick double-sided pressure sensitive adhesive (PSA) and (iii) bottom disc which is cut from a 0.5 mm thick clear PMMA sheet as shown in Fig. 1(a). The top layer has a round loading chamber cut into along with a venting channel that connects the detection chamber to the loading chamber for exchange of trapped air. The top layer also has a bead loading column with a channel and access hole for loading the beads. The middle layer has a channel connecting the loading chamber to the detection chamber for fluid flow. The bottom layer serves as the base and only has two alignment holes in it. Figure 1(b) shows a 3D model of the microfluidic structure after the disc has been assembled and Fig. 1(c) shows a schematic of the working principle of the disc. The features on the PMMA sheets were cut using a computer numerical control (CNC) milling machine (Roland Modela MDX-40A). The features on the PSA were cut using a cutter plotter (Graphtec CE6000-40). The three layers have alignment holes which were used to align and assemble the three layers after which the disc was left in a manual press overnight to ensure uniform bonding.

2.2. Bead packing in centrifugal microfluidic disc

The NBNM agarose beads were packed in the discs by first diluting the bead resin stock (Capto Adhere, Cytiva) in DI-water at 20% (v/v). 20 μL of the diluted bead stock solution was then added to each bead chamber on the disc and excess solution was manually pushed out from the outlet using a pipette. The disc was subsequently placed in a vacuum chamber (10 min, Femto Science CUTE, 15 Pa) to dehydrate the beads. After dehydration, the disc is ready to use.

2.3. Heating module

The heating module is made up of a custom designed ring-shaped printed circuit board (PCB) which serves as a heating element for contact-based heating of the disc. The PCB is made of aluminum having an outer diameter of 120 mm and inner diameter of 75 mm. There are 4 supporting structures having holes with a diameter of 3 mm to secure the heater on the platform using M3 screws and 2 circular conducting pads to connect it to the power supply. The PCB uses the principle of joule heating and has a conductor of length 4288 mm and width of 1 mm running from one end to the other like a winding structure. The conductor has a resistance of 3.2 Ω and a cross section of 0.03 mm^2. It has a power dissipation of 43W at a supply voltage of 12V. The PCB has a black silkscreen to allow for a plain background during the detection process as the centrifugal microfluidic discs are transparent. The power supply to the heater is controlled using a MOSFET combined with PID (proportional integrative derivative) control algorithm.

2.4. Signal acquisition using computer vision Raspberry Pi 4

The signal acquisition module uses a Raspberry Pi Camera Module 2 connected to a Raspberry Pi 4 computer. The camera module has an 8-megapixel sensor which is covered manually with a Kapton

(polyimide) film for fluorescence imaging working as an emission filter. The video feed from the camera is fed to the Raspberry Pi 4 computer where the computer vision algorithm detects the AruCo markers for each channel and then identifies the detection chamber using the AruCo marker as a reference and measures the RGB values inside the detection chamber. Based on the measured values and the defined threshold, the computer decides whether the sample is positive or negative. Figure S1 shows screenshots of the configuration panel in the software for computer vision algorithm and the different parameters that can be used for optimizing the detection procedure. Figure S2 shows screenshots of the computer vision-based detection algorithm detecting a positive and a negative signal.

2.5. RT-LAMP for SARS-CoV-2 RNA

The RT-LAMP was performed in a Mic® qPCR cycler (Biomolecular systems, Australia) with a total of 10 µL per reaction mixture. The reaction mixture containing 1 µL template RNA or spiked artificial saliva sample (Sigma Aldrich; Article# SAE0149) was prepared with final concentrations of 1X WarmStart LAMP Master Mix (New England Biolabs), 1X LAMP Fluorescent Dye (New England Biolabs) and 1X primer mix. The primer mixture at 10X concentration was prepared with 2 µM F and B, 16 µM FIP and BIP and 4 µM LF and LB. The As1e primer set reported by Rabe *et al.* was used. The As1e primer sequences were the following: F-5'-CGG TGG ACA AAT TGT CAC-3'; B-5'-CTT CTC TGG ATT TAA CAC ACT T-3'; FIP-5'-TCA GCA CAC AAA GCC AAA AAT TTA TTT TTC TGT GCA AAG GAA ATT AAG GAG-3'; BIP-5'-TAT TGG TGG AGC TAA ACT TAA AGC CTT TTC TGT ACA ATC CCT TTG AGT G-3'; LF-5'-TTA CAA GCT TAA AGA ATG TCT GAA CAC T-3'; LB-5'-TTG AAT TTA GGT GAA ACA TTT GTC ACG-3'. All primers were synthesized by Thermo Fisher Scientific. Synthetic fragments of SARS-CoV-2 RNA used to characterize and optimize LAMP were generated by (200–300 bp) by *in vitro* transcription of PCR fragments containing a part of SARS-CoV-2 sequence and T7 promoter as described elsewhere (Alekseenko et al., 2021).

2.6. Detection of SARS-CoV-2 RNA using the platform

The sample containing the RNA template (*in vitro* synthesized RNA fragment) was first combined with the LAMP master mix at a ratio of 10% (v/v) and 10 µL were subsequently added to the loading chamber in the disc. All the channels on the disc were sealed completely with a sheet of PSA (ARSeal™ 90880). The PSA sheet prevents evaporation of the solutions during LAMP and cross-contamination. The sealed disc was subsequently inserted into the slot and incubated, and further processing was carried out using an automated protocol. Initially the ring heating module is heated to achieve a temperature of 90°C and then the disc is brought in contact with the heater surface through the lifting mechanism controlled by a servo motor. As the disc comes in contact with the ring heater, the temperature inside the chamber starts to increase. The heater is maintained at 90°C for the initial 25 sec after which it is brought down and maintained at 65°C for 30 min. After 30 min, the disc is lifted to remove the contact from the heating surface and rotated at 1500 RPM for 1 minute to allow the flow of LAMP mix through the packed NBNM agarose beads. After 1 minute, the disc is rotated at 2 RPM for detection using computer vision.

3. Results and Discussion

3.1. Operation of the centrifugal microfluidic disc

The fabrication and assembly of the centrifugal microfluidic disc was already described in section 2.1. Figure 2(a) shows the image of an assembled disc having 26 channels allowing testing of 26 samples in one test. Figure 2 (i-iv) show the working of the microfluidic structure on the disc in a step-by-step manner. Figure 2(i) shows the initial stage when the sample has been loaded in the loading chamber. Figure 2(ii and iii) show the intermediate steps when the disc is rotating, and the liquid is being pushed from the loading chamber into the detection chamber passing through the bead chamber. As the liquid enters the detection chamber, the trapped air inside the detection chamber is pushed through the channel for air transfer into the loading chamber. As the volume of the liquid in the detection chamber increases, more and more of the air is transferred to the loading chamber. Figure 2(iv) shows the final state of the liquid in the microfluidic structure where the transfer between liquid and trapped air has completed.

3.2. Integrated centrifugal microfluidic platform

The integrated centrifugal microfluidic platform shown in Fig. 2 (b) has a dimension of 200 × 160 × 125 mm (L × W × H) which makes it very portable and easy to carry in the field. The top view of the platform shows the Raspberry Pi 4 computer which is used to control all the peripherals and attached sensors. The top view also shows the ring PCR heater in which is used to heat the disc. The side view of the platform shows the location of the camera which is used for the computer vision-based detection and the laser which is directed towards the detection chamber on the disc. The top and side view also the show the disc mounting structure in the middle of the PCB heater. The mounting structure has AruCo codes printed on it and it has two slots which serve as the guide to mount the disc by placing the matching tabs of the disc in the corresponding slots and locking the disc into position. Once the disc has been mounted securely, the mounting structure can be moved vertically using a lever which is moved through a servo motor underneath it. The mounting structure is attached to the shaft of a stepper motor which rotates the mounting structure and the disc along with it. As shown in Figure S3, passing the sample solution through the beads once is enough to remove the non-specific signal caused by intra- and inter- primer dimer hybridization. This has allowed the use of a stepper motor as it can go up to 2500 RPM and also able to rotate at very low RPM such as 1–2 RPM which is required for computer vision-based detection (Figure S3).

3.3. Heating module

The heating module consists of a ring-shaped PCB heater which works on the principle of Joule heating. A schematic of the conductor embedded inside the PCB is shown in Fig. 3(a). The conductor is designed in this way to maximize the length as the resistance of a conductor is directly proportional to the length. Figure 3(b) shows the temperature profile of the heater and the temperature inside the loading chamber of the disc. To minimize the time required to heat the reaction mixture to the desired temperature of 65°C, the heater is preheated to 90°C and kept at 90°C for 25 sec after contact with the disc before

allowing to cool down to 65°C. As shown in Fig. 3(b), the desired temperature is achieved inside the chamber in around 60 sec. After this, both the heater and the disc are maintained at 65°C for the remaining duration.

3.4. Characterization of the platform with dilution series in nuclease free water

The integrated centrifugal microfluidic platform was characterized by testing a dilution series of RNA fragments spiked in nuclease-free water, with results shown in Fig. 4. Figure 4(a) shows RT-LAMP amplification curves obtained on a benchtop Mic® qPCR cycler across the dilution series, confirming that the assay reliably amplifies template concentrations of 10^3 copies per reaction and above, with partial amplification observed at 10^2 copies (2 of 3 replicates positive). This benchtop characterization was used to define the assay's working range ahead of testing on the integrated platform. Figure 4(b) shows the results of the same dilution series tested end-to-end on the integrated platform, where detection provides a positive or negative call rather than an amplification curve. On the platform, all three replicates were positive at 10^3 copies per reaction, while all replicates at 10^2 copies were negative, giving a limit of detection of approximately 10^3 copies per reaction for the integrated platform in water.

3.5. Detection in artificial saliva samples

The integrated centrifugal microfluidic platform was similarly characterized using a dilution series of RNA fragments spiked in artificial saliva, with results shown in Fig. 5. Figure 5(a) shows RT-LAMP amplification curves obtained on the benchtop Mic® qPCR cycler, with amplification observed at 10^3 copies per reaction and only partial amplification at 10^2 copies (1 of 3 replicates positive), consistent with the modest reduction in sensitivity typically associated with the more complex saliva matrix. Figure 5(b) shows the results of the same dilution series tested end-to-end on the integrated platform. Both replicates tested were positive at 10^3 copies per reaction, while replicates at 10^2 copies were negative, giving a limit of detection of approximately 10^3 copies per reaction on the integrated platform in artificial saliva, consistent with the result obtained in water. As only two replicates were tested in the saliva dilution series on the platform, this result should be considered preliminary and would benefit from additional replicates in future work.

Conclusion

We present a fully automated centrifugal microfluidic platform for sample-to-answer molecular diagnostics, combining our previously reported bead-based signal enhancement strategy (Soares et al., 2021) with loop-mediated isothermal amplification (LAMP) and computer-vision-based readout, demonstrated here using artificial saliva samples for SARS-CoV-2 detection. The platform uses centrifugal microfluidic discs capable of processing 26 samples in parallel. After loading the samples and mounting the disc, the heating, rotation, and detection process is carried out automatically, and the user can view the results directly on the screen. Compared to our previous work, this new platform

provides several advantages: (i) a lower rotational speed requirement, (ii) lower power consumption due to the disc geometry and single-sided heating, and (iii) a simpler readout based on signal measurement at a defined position using computer vision. These improvements have produced a fully automated platform suitable for point-of-care diagnostics and pave the way for a battery-operated system for field use in resource-limited settings without reliable power infrastructure. While demonstrated here for SARS-CoV-2, the platform architecture is not specific to this target and can be readily adapted to other LAMP-compatible assays, offering a generalizable tool for decentralized diagnostics beyond the current pandemic context.

Declarations

Competing interest

The authors declare that they have no competing financial interests or personal relationships that could have appeared to influence the work reported in this paper.

Author Contribution

Conceptualization: A.A, N.L, A.R.; Methodology: A.A, N.L, J.M, L.P, A.P, F.M, D.M; Investigation: A.A, N.L; Software: J.M, L.P, A.P, F.M, D.M; Visualization: A.A; Writing – original draft: A.A; Writing – review & editing: A.A, I.P, A.R; Supervision: I.P, M.M, A.R; Funding acquisition: A.R.

Acknowledgement

This work has been sponsored by the European Union's Horizon Europe research and innovation programme "HoliCare" under grant agreement No. 101057596. We would like to thank Donal Barrett for providing the in vitro transcribed synthetic RNA fragments.

References

1. ABDELFATAH, T., JALALI, M., YEDIRE, S. G., I. HOSSEINI, I., DEL REAL MATA, C., KHAN, H., HAMIDI, S. V., JEANNE, O., SIAVASH MOAKHAR, R., MCLEAN, M., PATEL, D., WANG, Z., MCKAY, G., YOUSEFI, M., NGUYEN, D., VIDAL, S. M., LIANG, C. & MAHSHID, S. 2023. Nanoplasmonic amplification in microfluidics enables accelerated colorimetric quantification of nucleic acid biomarkers from pathogens. *Nature Nanotechnology,* 18**,** 922-932.
2. ALEKSEENKO, A., BARRETT, D., PAREJA-SANCHEZ, Y., HOWARD, R. J., STRANDBACK, E., AMPAH-KORSAH, H., ROVSNIK, U., ZUNIGA-VELIZ, S., KLENOV, A., MALLOO, J., YE, S., LIU, X., REINIUS, B., ELSASSER, S. J., NYMAN, T., SANDH, G., YIN, X. & PELECHANO, V. 2021. Direct detection of SARS-CoV-2 using non-commercial RT-LAMP reagents on heat-inactivated samples. *Sci Rep,* 11**,** 1820.

3. BI, Q., LIU, M., YAN, L., CHENG, J., SUN, Q., DAI, Y. & ZOU, L. 2025. Progress in the application of isothermal amplification technology in the diagnosis of infectious diseases. *Front Microbiol,* 16**,** 1601644.
4. BYANYIMA, P., KASWABULI, S., MUSISI, E., NABAKIIBI, C., ZAWEDDE, J., SANYU, I., SESSOLO, A., ANDAMA, A., WORODRIA, W., HUANG, L. & DAVIS, J. L. 2022. Feasibility and Sensitivity of Saliva GeneXpert MTB/RIF Ultra for Tuberculosis Diagnosis in Adults in Uganda. *Microbiology Spectrum,* 10**,** e00860-22.
5. CHAKRABORTY, S. 2024. Democratizing nucleic acid-based molecular diagnostic tests for infectious diseases at resource-limited settings – from point of care to extreme point of care. *Sensors & Diagnostics,* 3**,** 536-561.
6. CUNHA, M. L., DA SILVA, S. S., STRACKE, M. C., ZANETTE, D. L., AOKI, M. N. B. & BLANES, L. 2021. Sample Preparation for Lab-on-a-Chip Systems in Molecular Diagnosis: A Review. *Analytical Chemistry,* 94**,** 41-58.
7. HERNAEZ, B., MUñOZ-GóMEZ, A., SANCHIZ, A., ORVIZ, E., VALLS-CARBO, A., SAGASTAGOITIA, I., AYERDI, O., MARTíN, R., PUERTA, T., VERA, M., CABELLO, N., VERGAS, J., PRIETO, C., PARDO-FIGUEREZ, M., NEGREDO, A., LAGARóN, J. M., DEL ROMERO, J., ESTRADA, V. & ALCAMí, A. 2023. Monitoring monkeypox virus in saliva and air samples in Spain: a cross-sectional study. *The Lancet Microbe,* 4**,** e21-e28.
8. JENKINS, H. H., LOPEZ, A. A. T., TARANTINI, F. S., TOMLIN, H., SCALES, D., LEE, I. N., WU, S., HYDE, R., LIS-SLIMAK, K., BYARUHANGA, T., THOMPSON, J. L., PIJUAN-GALITO, S., DOOLAN, L., KANEKO, K., GWYNNE, P., REFFIN, C., PARK, E., DEY, J., HILL, J., ARENDT-TRANHOLM, A., STROUD, A., PETRIE, M., DENNING, C., BENEST, A. V. & SEEDHOUSE, C. 2022. Performance evaluation of a non-invasive one-step multiplex RT-qPCR assay for detection of SARS-CoV-2 direct from saliva. *Scientific Reports,* 12**,** 11553.
9. JIRAKITTIWUT, N. & RATTHAWONGJIRAKUL, P. 2025. Advances in Isothermal Amplification for the Diagnosis of Tuberculosis. *J Clin Lab Anal,* 39**,** e70113.
10. JUSTO, C. A. C., JAUSET-RUBIO, M., SKOURIDOU, V., COOLS, P., HIMSCHOOT, L., NEGASH, A. A., MULINGANYA MULUMEODERHWA, G., IBÁÑEZ-ESCRIBANO, A. & O'SULLIVAN, C. K. 2025. Development of a Protein-Free Nucleic Acid Lateral Flow Assay for Trichomonas vaginalis. *Analytical Chemistry,* 97**,** 15093-15103.
11. KSHIRSAGAR, A., DEROSA, D., POLITZA, A. J., LIU, T., DONG, M. & GUAN, W. 2025. Point-of-need one-pot multiplexed RT-LAMP test for detecting three common respiratory viruses in saliva. *Biosensors and Bioelectronics,* 288**,** 117836.
12. KUMARI, S., SAMARA, M., AMPADI RAMACHANDRAN, R., GOSH, S., GEORGE, H., WANG, R., PESAVENTO, R. P. & MATHEW, M. T. 2023. A Review on Saliva-Based Health Diagnostics: Biomarker Selection and Future Directions. *Biomed Mater Devices***,** 1-18.
13. LEE, U. N., SU, X., HIEBER, D. L., TU, W.-C., MCMANAMEN, A. M., TAKEZAWA, M. G., HASSAN, G. W., CHAN, T. C., ADAMS, K. N., WALD, E. R., DEMURI, G. P., BERTHIER, E., THEBERGE, A. B. &

THONGPANG, S. 2022. CandyCollect: at-home saliva sampling for capture of respiratory pathogens. *Lab on a Chip,* 22**,** 3555-3564.

14. LU, X., DU, J., YOU, M., CHEN, L., XU, F. & CHEN, F. 2025. From crisis to innovation in point-of-care testing: Lessons from the COVID-19 pandemic and future directions. *TrAC Trends in Analytical Chemistry,* 184.
15. MARGULIS, M., ROHANA, H., ERSTER, O., MANDELBOIM, M., BIBER, A., SCHWARTZ, E., PERETZ, A. & DANIELLI, A. 2024. Highly sensitive extraction-free saliva-based molecular assay for rapid diagnosis of SARS-CoV-2. *Journal of Clinical Microbiology,* 62**,** e00600-24.
16. NARASIMHAN, V., KIM, H., LEE, S. H., KANG, H., SIDDIQUE, R. H., PARK, H., WANG, Y. M., CHOO, H., KIM, Y. & KUMAR, S. 2023. Nucleic Acid Amplification-Based Technologies (NAAT)—Toward Accessible, Autonomous, and Mobile Diagnostics. *Advanced Materials Technologies,* 8**,** 2300230.
17. NOVI, V. T., MEHER, A. K. & ABBAS, A. 2025. Visualization methods for loop mediated isothermal amplification (LAMP) assays. *Analyst,* 150**,** 588-599.
18. PEELING, R. W. & SIA, S. K. 2023. Lessons from COVID-19 for improving diagnostic access in future pandemics. *Lab Chip,* 23**,** 1376-1388.
19. PENO, C., LIN, T.-Y., HISLOP MAIKEL, S., YOLDA-CARR, D., FARJADO, K., YORK, A., PITZER VIRGINIA, E., WEINBERGER DANIEL, M., BEI AMY, K., ALLICOCK ORCHID, M. & WYLLIE ANNE, L. 2024. A low-cost culture- and DNA extraction-free method for the molecular detection of pneumococcal carriage in saliva. *Microbiology Spectrum,* 12**,** e00591-24.
20. RAKEMAN-CAGNO, J. L., PERSING, D. H. & LOEFFELHOLZ, M. J. 2024. Maintaining point of care testing capacity and pandemic preparedness in the post-COVID-19 era. *Expert Rev Mol Diagn,* 24**,** 147-151.
21. RUTTER, H., WABNITZ, K., NAMBIAR, D., GARDE, A., BENTON, T. G., HEYMANN, D. L., YATES, R., FRIEL, S., HOLLANDS, G. J., CAI, W., CHATER, N., BLOOM, D. E., GUINTO, R. R., EL OMRANI, O., WILSDON, J., AMUASI, J. H., BUTLER, C., TLOU, S. & MARTEAU, T. M. 2026. The Lancet Commission on improving population health post-COVID-19. *Lancet,* 407**,** 267-308.
22. SOARES, R. R. G., AKHTAR, A. S., PINTO, I. F., LAPINS, N., BARRETT, D., SANDH, G., YIN, X., PELECHANO, V. & RUSSOM, A. 2021. Sample-to-answer COVID-19 nucleic acid testing using a low-cost centrifugal microfluidic platform with bead-based signal enhancement and smartphone read-out. *Lab on a Chip,* 21**,** 2932-2944.
23. SRITONG, N., NGO, W. W., EJENDAL, K. F. K. & LINNES, J. C. 2024. Development of an integrated sample amplification control for salivary point-of-care pathogen testing. *Analytica Chimica Acta,* 1287**,** 342072.
24. TANG, P., LIU, R., QIN, L., XU, P., XIONG, Y., DENG, Y., LV, Z., SHANG, Y., GAO, X., YAO, L., ZHANG, R., FENG, Y., DING, C., JING, H., LI, L., TANG, Y. W. & PANG, Y. 2023. Accuracy of Xpert(R) MTB/RIF Ultra test for posterior oropharyngeal saliva for the diagnosis of paucibacillary pulmonary tuberculosis: a prospective multicenter study. *Emerg Microbes Infect,* 12**,** 2148564.

25. TUPPS, C., CURRY, D., EDWARDS, A., BAZANT, E., MOEN, A., MOUNTS, A. W. & BRESEE, J. 2025. COVID-19 vaccination implementation in six lower- and middle-income countries: Successes, challenges, and lessons for pandemic preparedness. *PLOS Glob Public Health,* 5**,** e0004417.
26. VARUGHESE, J. E., JACOB, A. A., THAMPI, A., JOHN, J. J., DAVID, A., JOHN, G. M. & CHERUPANAKKAL, C. 2025. Utility of Saliva for Detecting Influenza A Virus by Cost-Effective Extraction-Free SYBR Green-Based PCR. *Journal of Medical Virology,* 97**,** e70475.
27. VOGELS, C. B. F., WATKINS, A. E., HARDEN, C. A., BRACKNEY, D. E., SHAFER, J., WANG, J., CARABALLO, C., KALINICH, C. C., OTT, I. M., FAUVER, J. R., KUDO, E., LU, P., VENKATARAMAN, A., TOKUYAMA, M., MOORE, A. J., MUENKER, M. C., CASANOVAS-MASSANA, A., FOURNIER, J., BERMEJO, S., CAMPBELL, M., DATTA, R., NELSON, A., ANASTASIO, K., ASKENASE, M. H., BATSU, M., BICKERTON, S., BROWER, K., BUCKLIN, M. L., CAHILL, S., CAO, Y., COURCHAINE, E., DEIULIIS, G., EARNEST, R., GENG, B., GOLDMAN-ISRAELOW, B., HANDOKO, R., KHOURY-HANOLD, W., KIM, D., KNAGGS, L., KUANG, M., LAPIDUS, S., LIM, J., LINEHAN, M., LU-CULLIGAN, A., MARTIN, A., MATOS, I., MCDONALD, D., MINASYAN, M., NAKAHATA, M., NAUSHAD, N., NOUWS, J., OBAID, A., ODIO, C., OH, J. E., OMER, S., PARK, A., PARK, H.-J., PENG, X., PETRONE, M., PROPHET, S., RICE, T., ROSE, K.-A., SEWANAN, L., SHARMA, L., SHAW, A. C., SHEPARD, D., SMOLGOVSKY, M., SONNERT, N., STRONG, Y., TODEASA, C., VALDEZ, J., VELAZQUEZ, S., VIJAYAKUMAR, P., WHITE, E. B., YANG, Y., DELA CRUZ, C. S., KO, A. I., IWASAKI, A., KRUMHOLZ, H. M., MATHEUS, J. D., HUI, P., LIU, C., FARHADIAN, S. F., SIKKA, R., WYLLIE, A. L. & GRUBAUGH, N. D. 2021. SalivaDirect: A simplified and flexible platform to enhance SARS-CoV-2 testing capacity. *Med,* 2**,** 263-280.e6.
28. WANG, J., JIANG, H., PAN, L., GU, X., XIAO, C., LIU, P., TANG, Y., FANG, J., LI, X. & LU, C. 2023. Rapid on-site nucleic acid testing: On-chip sample preparation, amplification, and detection, and their integration into all-in-one systems. *Frontiers in Bioengineering and Biotechnology,* Volume 11 - 2023.
29. WONG, W. C., LIN, V., FANG, X., KIDD, M. & LANCET COMMISSION ON TRANSFORMING PRIMARY HEALTH CARE IN THE POST, C.-E. 2025. The Lancet Commission on Transforming Primary Health Care in the Post-COVID-19 Era. *Lancet,* 405**,** 527-528.
30. YIMER, S. A., BOOIJ, B. B., TOBERT, G., HEBBELER, A., OLOO, P., BRANGEL, P., L'AZOU JACKSON, M., JARMAN, R., CRAIG, D., AVUMEGAH, M. S., MANDI, H., ENDY, T., WOODEN, S., CLARK, C., BERNASCONI, V., SHURTLEFF, A. & KRISTIANSEN, P. A. 2024. Rapid diagnostic test: a critical need for outbreak preparedness and response for high priority pathogens. *BMJ Glob Health,* 9.
31. ZHANG, Z., PANDEY, R., LI, J., GU, J., WHITE, D., STACEY, H. D., ANG, J. C., STEINBERG, C.-J., CAPRETTA, A., FILIPE, C. D. M., MOSSMAN, K., BALION, C., MILLER, M. S., SALENA, B. J., YAMAMURA, D., SOLEYMANI, L., BRENNAN, J. D. & LI, Y. 2021. High-Affinity Dimeric Aptamers Enable the Rapid Electrochemical Detection of Wild-Type and B.1.1.7 SARS-CoV-2 in Unprocessed Saliva. *Angewandte Chemie International Edition,* 60**,** 24266-24274.

Figures

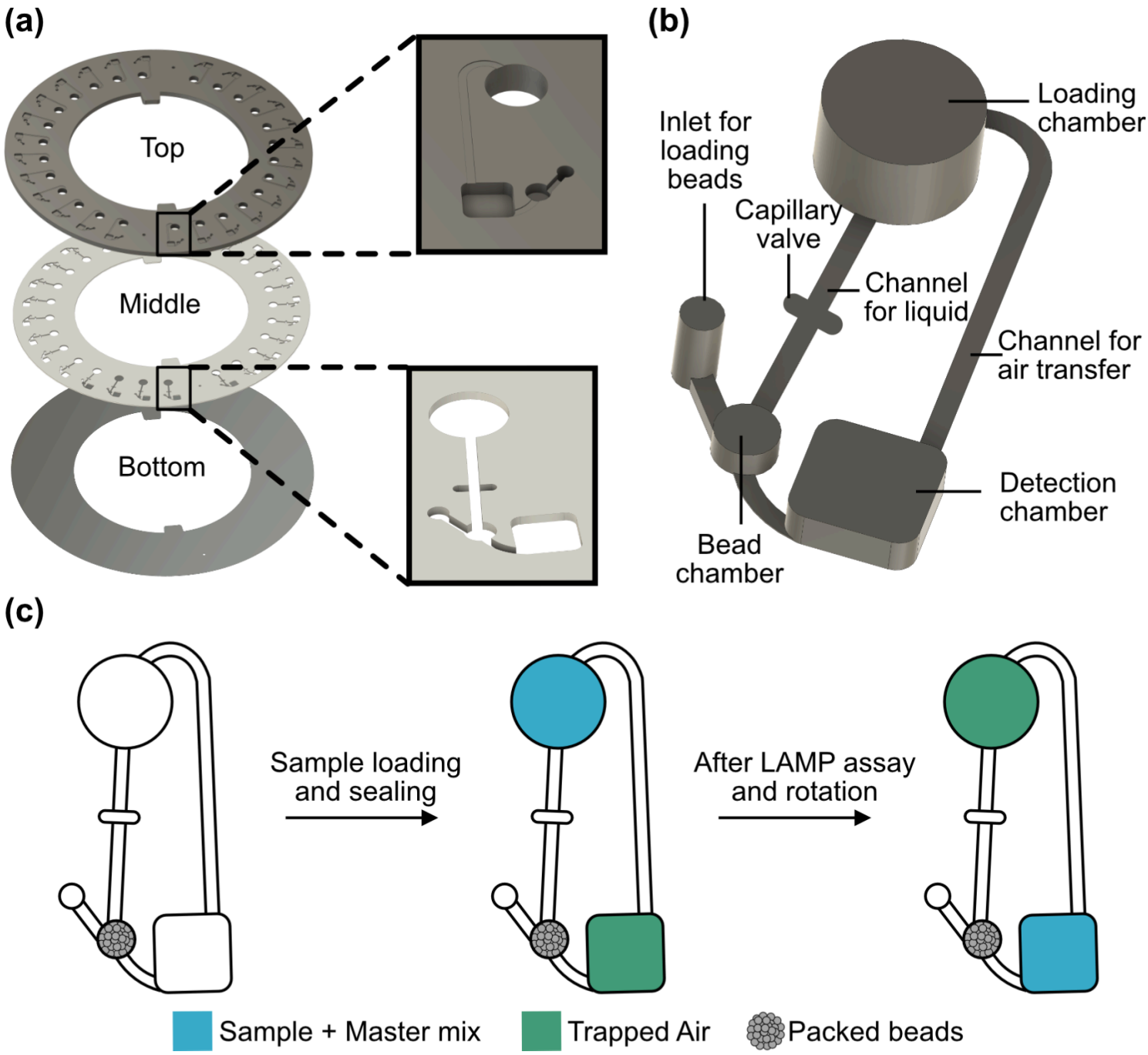


Figure 1

(a) Assembly of the centrifugal microfluidic disc showing the top, middle and bottom layer with a zoomed in image of structure on each layer. (b) A 3D model of the microfluidic structure after the disc has been assembled. (c) Schematics of the working principle of the microfluidic structure demonstrating how the exchange between the sample and trapped air takes place.

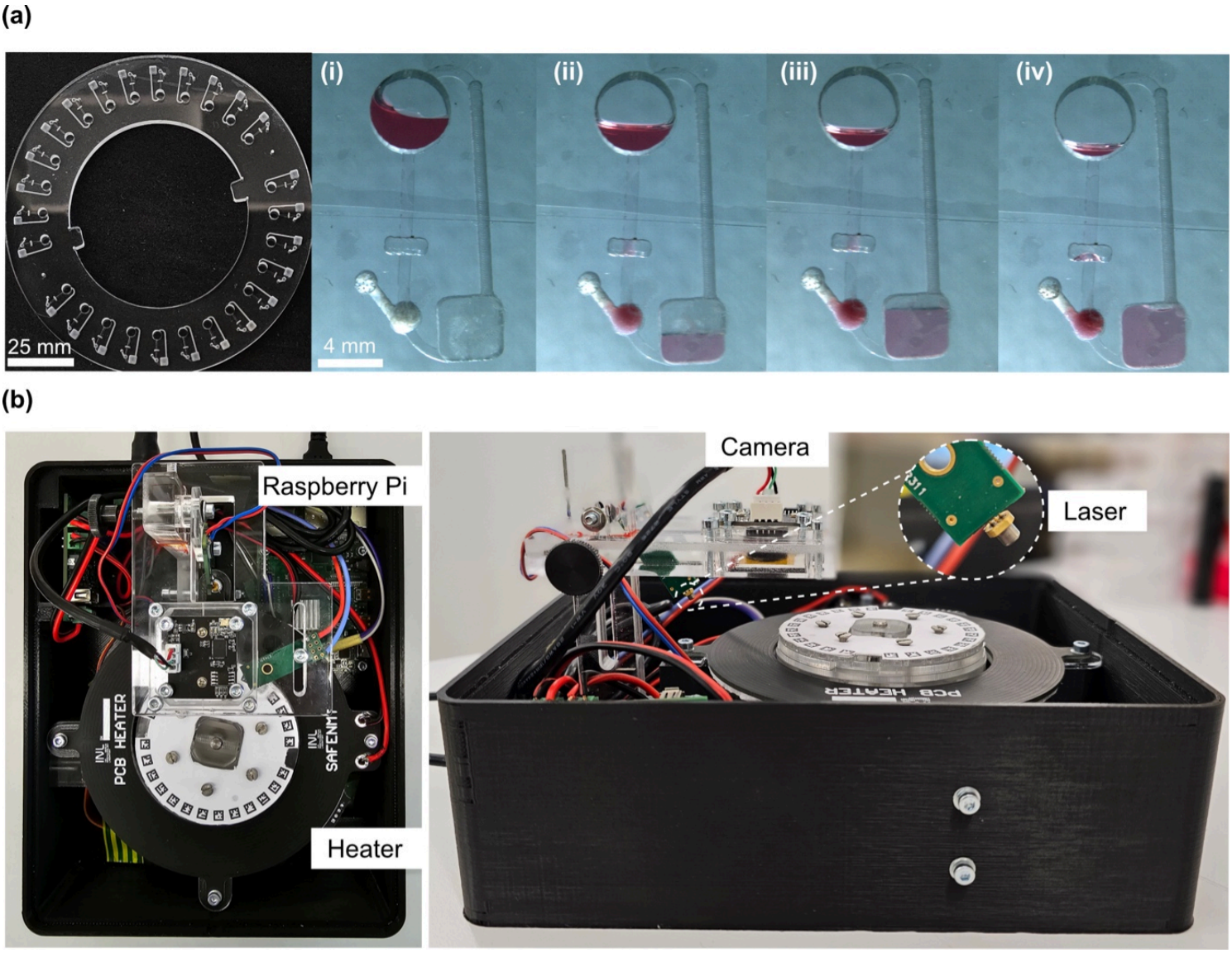


Figure 2

(a) Image of the assembled disc having 26 microfluidic structures. (i-iv) Demonstration of fluid flow in the microfluidic structure using a food dye mixed in water for visualization purposes. The sequential images show how the fluid from the loading chamber moves into the detection chamber and replaces the trapped air which moves into the loading chamber. (b) Top view (left) and side view (right) of the integrated centrifugal microfluidic platform showing the different components.

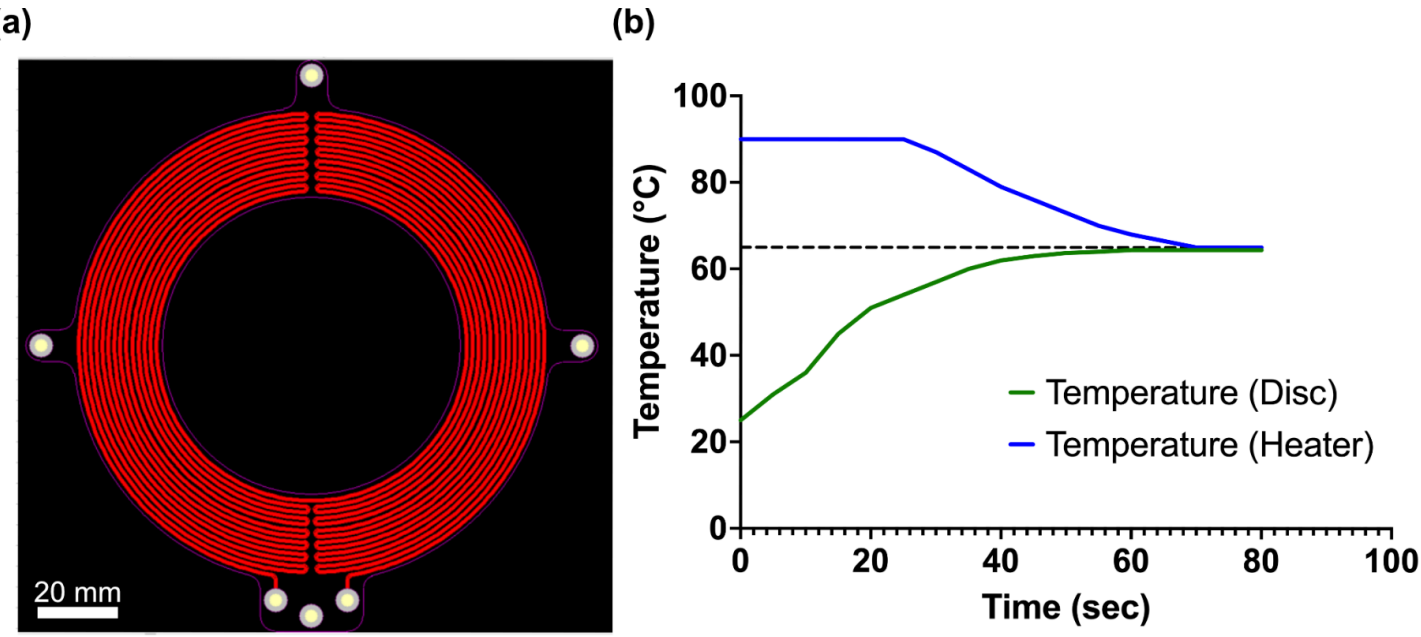
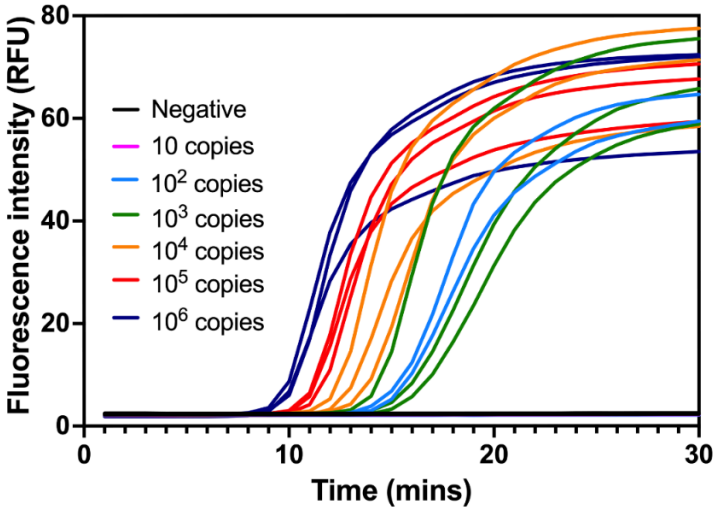


Figure 3

(a) Schematics of the conductor embedded inside the ring-shaped PCB heater. (b) The temperature profile of the PCB heater and the chamber inside the disc as the disc gets heated.

(a)



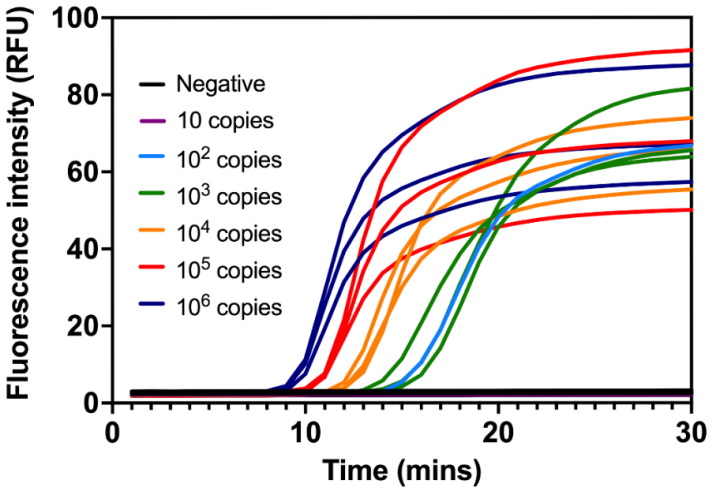
(b)

Target conc. (copies/reaction)	Replicate 1	Replicate 2	Replicate 3
Negative	–	–	–
10 copies	–	–	–
10^2 copies	–	–	–
10^3 copies	+	+	+
10^4 copies	+	+	+
10^5 copies	+	+	+
10^6 copies	+	+	+

Figure 4

(a) Dilution series of SARS-CoV-2 RNA fragment spiked in nuclease free water tested in Mic® qPCR cycler. (b) Dilution series of SARS-CoV-2 RNA fragment spiked in nuclease free water tested in the integrated centrifugal microfluidic platform.

(a)



(b)

Target conc. (copies/reaction)	Replicate 1	Replicate 2
Negative	–	–
10 copies	–	–
10^2 copies	–	–
10^3 copies	+	+
10^4 copies	+	+
10^5 copies	+	+
10^6 copies	+	+

Figure 5

(a) Dilution series of SARS-CoV-2 RNA fragment spiked in artificial saliva samples tested in Mic® qPCR cycler. (b) Dilution series of SARS-CoV-2 RNA fragment spiked in artificial saliva samples tested in the integrated centrifugal microfluidic platform.

Supplementary Files

This is a list of supplementary files associated with this preprint. Click to download.

- 02Supplementary.docx